Available online at www.sciencedirect.com

ScienceDirect

Biochimica et Biophysica Acta 1778 (2008) 133–142

Biochimica et Biophysica Acta BBA

www.elsevier.com/locate/bbamem

Interaction of ferredoxin:NADP$^+$ oxidoreductase with model membranes

Joanna Grzyb [a,1], Mariusz Gagoś [b], Wiesław I. Gruszecki [c], Monika Bojko [a], Kazimierz Strzałka [a,*]

[a] *Department of Plant Physiology and Biochemistry, Faculty of Biochemistry, Biophysics and Biotechnology, Jagiellonian University, ul. Gronostajowa 7, 30-387 Krakow, Poland*

[b] *Department of Physics, Agricultural University, Lublin, Poland*

[c] *Department of Biophysics, Maria Sklodowska-Curie University, Lublin, Poland*

Received 28 May 2007; received in revised form 17 August 2007; accepted 17 September 2007
Available online 5 October 2007

Abstract

The ferredoxin:NADP$^+$ oxidoreductase (FNR) is a plant enzyme, catalyzing the last step of photosynthetic linear electron transport, and involved also in cyclic electron transport around photosystem I. In this study we present the first evidence of FNR (isolated from spinach and from wheat) interaction directly with a model membrane without the mediation of any additional protein. The monomolecular layer technique measurements showed a significant increase in surface pressure after the injection of enzyme solution beneath a monolayer consisting of chloroplast lipids: monogalactosyldiacylglycerol or digalactosyldiacylglycerol. An ATR FTIR study revealed also the presence of FNR in a bilayer composed of these lipids. The secondary structure of the protein was significantly impaired by lipids, as with a pH-induced shift. The stabilization of FNR in the presence of lipids leads to an increase in the rate of NADPH-dependent reduction of dibromothymoquinone catalyzed by the enzyme. The biological significance of FNR–membrane interaction is discussed.

Keywords: Ferredoxin:NADP+ oxidoreductase; Fourier transform infrared spectroscopy; Isoform; Model membrane; Monomolecular lipid layer; Photosynthesis

1. Introduction

Ferredoxin:NADP$^+$ oxidoreductase (FNR, E.C 1.18.1.2) is a plant enzyme present in photosynthetic and non-photosynthetic tissues. In chloroplasts, FNR catalyses the last step of the photosynthetic electron transport chain, carrying electrons from ferredoxin (Fd) to NADP$^+$, which results in the formation of NADPH [1]. In roots, an FNR isoform catalyses a back reaction, carrying electrons from NADPH to reduce Fd, which is essential for the biosynthesis of lipids, nitrogen assimilation, and other processes [2].

Isolated and crystallized FNR is a monomer of about 36 kDa, consisting of two domains, a C-terminal, on NADP-binding domain, and the N-terminal part of FNR molecule, which is responsible for FAD binding. The NADP binding domain has a dehydrogenase conserved motif, β–α–β, while the FAD binding domain consists mainly of β-sheet [1]. Fd is supposed to be bound to the region of the interdomain space [3], but the flexible N-terminus of FNR has been shown to be also important in this interaction [4]. The catalytic activity of FNR is ensured by Ser 96, Glu 312 and Tyr 314 (numeration for spinach protein). The tyrosine residue, placed parallel to FAD moiety, enables proton transfer to NADP$^+$ [5]. Ser 96 provides the correct orientation of the electron pair on N-5 of the isoalloxasine ring of FAD, facilitating the transfer of a proton from water-exposed Glu 312 [6]. After the formation of the FNR–Fd complex, a hydrogen bond between Ser 96 and Glu 312 is created [3].

Isoforms of FNR from photosynthetic and non-photosynthetic tissues are products of different genes. However, in leaves also the presence of FNR isoforms being products of different genes has been shown [7–9]. The isoproteins differ in their molecular weight by about 1–3 kDA, but differences in their theoretical isoelectric points are more distinct. pI approximates about 5 for isoform called “acidic” and between 7 and 8 for “basic” form of the enzyme [9]. In vivo, FNR binds to PSI via a

* Corresponding author. Tel./fax: +48 12 664 6902.
E-mail address: strzalka@mol.uj.edu.pl (K. Strzałka).
[1] Present address: Department of Plant Sciences, Weizmann Institute of Science, Rehovot, Israel.

0005-2736/$ - see front matter © 2007 Published by Elsevier B.V.
doi:10.1016/j.bbamem.2007.09.028

17.5-kDa reductase binding protein [10], or the PsaE subunit of PSI [11,12]. FNR was also co-purified with a thylakoidal cytochrome b_6f complex [13] and on NAD(P)H dehydrogenase complex [14]. It has been postulated that connectein, a protein of about 10 kDa, might create a complex with FNR at a ratio of 1:2 [15,16]. Recently, a pH- and ionic strength dependent oligomerisation of wheat FNR has been shown in vitro [17].

Apart from playing a role in photosynthetic linear electron transfer, FNR from chloroplasts is postulated to be involved in cyclic electron transfer around PSI. This process occurs at a maximal rate when PSII is blocked e.g. as a result of photoinhibition, or there is no $NADP^+$ for reduction but a transthylakoidal gradient must be generated to support the activity of ATP synthase [18]. It has been shown in an in vitro system that FNR has an ability to reduce quinones, both artificial, such as dibromothymoquinone (DBMIB) [19–21] and natural, as plastoquinones [22]. A difference in the location of the quinone binding site and other substrate binding sites on FNR molecule was proved in studies with monoclonal antibodies [23] and inhibitors [21].

Quinones with a long acyl chain, such as natural plastoquinone 9 (PQ-9) might be effectively reduced only if presented to the FNR in the correct orientation. In vitro it is facilitated by detergent micelles, such as sodium cholate [22]. However, up to now there was no evidence whether FNR could interact directly with lipid molecules. Hence, the aim of our study was to clarify this issue. Two main lipids of thylakoid membranes, the monogalactosyldiacylglycerol (MGDG) and digalactosyldiacylglycerol (DGDG), have been chosen because they form a natural environment for FNR binding. The structures created by both lipids in a water environment are determined by the ratio of the polar head group size and hydrophobic tail dimension. DGDG, where the cross-sectional area of the headgroup and the cross-sectional area of acyl chains are not very different, creates a bilayer in a water environment, while the reverse hexagonal phase (H_{II}) is formed by MGDG, where the cross-sectional area of the polar headgroup is smaller than that of acyl chains [24]. These differences are of great importance *in vivo*. It has been shown that H_{II} domains facilitate violaxanthin conversion to antheraxanthin and zeaxanthin by violaxanthin de-epoxidase, the xanthophyll cycle enzyme [25,26] and diadinoxanthin to diatoxanthin transformation by diadinoxanthin de-epoxidase in the diadinoxanthin cycle [26,27]. It is also believed that H_{II} phase, due to more free space between polar head groups on the external surface, facilitates protein incorporation into the membrane, and induces conformational changes of these proteins [28].

The monomolecular layer at the air–water interphase as well as model lipid bilayers are widely used tools to investigate the incorporation or interaction of various molecules with the lipid membrane [29–32]. Here we demonstrate that FNR from spinach and from wheat may bind to a membrane composed of MGDG or DGDG. The rate of binding depends on the pH, which is most probably connected with the conformation of the protein and not the lipid type. The interaction with lipids influenced the secondary structure of FNR, as shown by ATR FTIR and circular dichroism (CD). The enzymatic activity of FNR was significantly altered upon contact with lipids.

2. Materials and methods

2.1. Isolation and purification of FNRs

Spinach FNR was isolated by a method described in [19]. Fresh spinach leaves were obtained on the local market. Wheat FNR was isolated from 7-day-old wheat leaves by the method described in [17]. Wheat was grown in a hydroponic culture in a growing chamber, with fotoperiod 8 h dark/16 h light. Both FNR preparations were of electrophoretic purity. Spinach FNR consisted of protein of 36 kDa and a smaller amount of the 33-kDa protein, the product of a partial proteolytic degradation of FNR [33]. The wheat FNR preparation was a complex of two isoforms of the enzyme present in the leaves and differing in pI values. The dominating form (as tested by native electrophoresis) was an isoform of pI near 5.

2.2. Monomolecular layers on air–water interphase

2.2.1. Monolayers of lipids

The lipid monolayers were formed from 20 µl of chloroform stock solution of lipids (DGDG or MGDG, 5 mM).The water phase was buffered with a 25-mM phosphate buffer pH 5.2 or 7.0, or 25 mM HEPES/NaOH buffer pH 7.0 or 8.0, and gently stirred with a magnetic stirrer all the time. The volume of the buffer in a Teflon dish was 12 ml. Surface pressure was monitored by a NIMA Technology tensiometer, model PS3 (Coventry, UK). Starting conditions were usually set at 20 mN/m. The FNR solution was injected by Hamilton syringe beneath the monolayer. The changes in the surface pressure were monitored and recorded every 3 s by a computer connected to a tensiometer. The whole set – the dish and the tensiometer – was closed in a box filled with argon atmosphere. Relative humidity was 100%.

To compare lipid properties at differing pH, the isoterms of compression for pure lipids were additionally recorded. The water phase, filling the Teflon trough (40 cm × 4 cm), was buffered with a 25-mM phosphate buffer pH 7.0 or 5.2. The monolayers were formed by a slow deposition of DGDG or MGDG stock solutions on the surface of the water phase. After evaporation of chloroform, the monolayer was compressed along the long side at a speed of 5 mm/min. Changes in the surface pressure were monitored and recorded every 3 s by a computer connected to the tensiometer.

2.2.2. Monolayers of protein

The water phase filling the Teflon trough (40 cm × 4 cm) was buffered with a 25-mM phosphate buffer pH 7.0 or 5.2. The monolayers were formed by a slow deposition of an FNR stock solution (100 µl as a few drops) on the surface of the water phase, and were compressed along the long side at a speed of 5 mm/min. The changes in the surface pressure were monitored and recorded every 3 s by a computer connected to the tensiometer.

2.3. Bilayers

The bilayer of lipids was formed between the water surface (buffered with 25 mM HEPES/NaOH pH 7.0 or 8.2) and the surface of Ge crystal by the "attach" technique [31,32]. The equipment used enabled a controlled shifting of Ge. A dish was filled with 12.3 ml of buffer, and a volume of 25 µl of DGDG, 5 mM chloroform stock solution, was deposited to obtain $\pi = 20$ mN/m (previously tested using the tensiometer). The Ge crystal was shifted to touch the monolayer, and picked up. A second volume of 10 µl of DGDG stock solution

Table 1
Characteristics of C–H stretching vibrations in CH_2 and CH_3 groups of DGDG bilayer

Bilayer composition	Vibration	Band position [cm^{-1}]	Dichroic ratio R	S	α [deg]	θ [deg]
DGDG	$\nu_s(CH_2)$	2850	1.18	0.57	90	32
	$\nu_{as}(CH_2)$	2918	1.25	0.49		35
	$\nu_s(CH_3)$	2870	1.40	−0.17	0	62
	$\nu_{as}(CH_3)$	2956	1.55	−0.10		59

was added to obtain again π=20 mN/m and the Ge crystal, with deposited first monolayer was shifted down, to form the bilayer. The quality of bilayer formed was checked with dichroic ratio (Table 1). FNR was injected beneath the bilayer with a Hamilton syringe. The FTIR spectra of the bilayer were recorded after injection and during following 10 min periods, in the range of 400–4000 cm^{-1}, with a resolution of 4 cm^{-1}. 36 scans were accumulated, Fourier transformed and averaged. As a background, a spectrum just after injection of FNR was recorded (time zero). For linear dichroism, the ZnSe Infrared Polarizer (Pike Technologies, USA) was used.

2.4. FTIR spectra of FNR partially hydrated film

20 µl of 33 µM FNR stock solution (in 40 mM Tris/HCl pH 7.5) was concentrated on ZnSe crystal with a gentle stream of nitrogen. Final drying was done in stream of argon, filling FTIR spectrometer (Vektor 33, Bruker, Inc). FTIR spectra were recorded in the range of 400–4000 cm^{-1}, with resolution 1 cm^{-1} and 36 scans accumulated. As the background, a spectrum of clean crystal was used.

2.5. Liposome preparation

Small unilamellar liposomes (SUV) were formed from multilamellar liposomes (MLV). For this purpose, a chloroform stock solution of DGDG, or a mixture MGDG:DGDG (30 mol% of MGDG) were placed in a glass tube, dried with a stream of nitrogen and placed under vacuum for 1 h. Then, a 25-mM HEPES buffer, pH 8.2 was added, and the tube was shaken with Vortex for 4–5 min. The MLV were sonicated for 10 min (P=20 W, Ultrasonic homogenizer, Cole Plamer Instruments, USA) and SUV were created (manifested by the change from a white suspension to an opalising, colorless solution). The final concentration of lipids in liposome preparation was 1.4 mM.

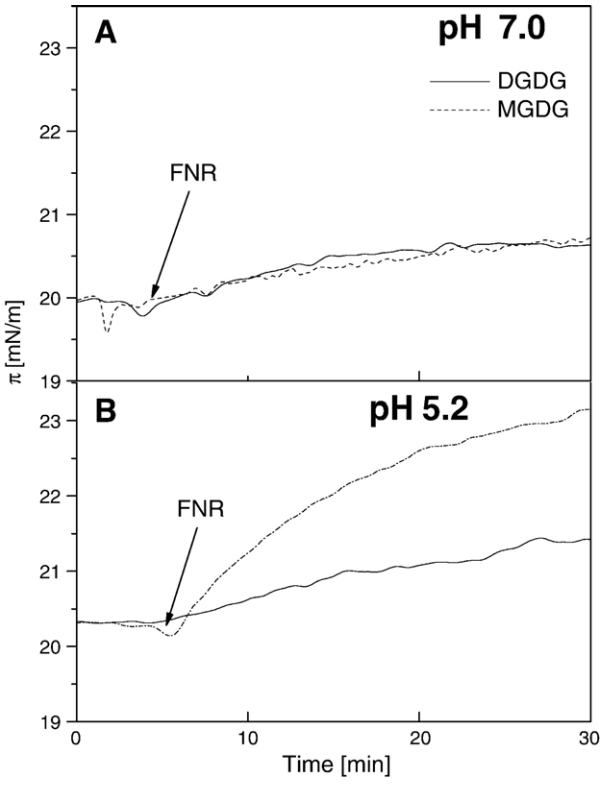

Fig. 1. Effect of pH on interaction between spinach FNR and MGDG or DGDG monolayer (air–water interphase), as monitored by changes in the surface pressure. A—pH 7.0, B—pH 5.2.

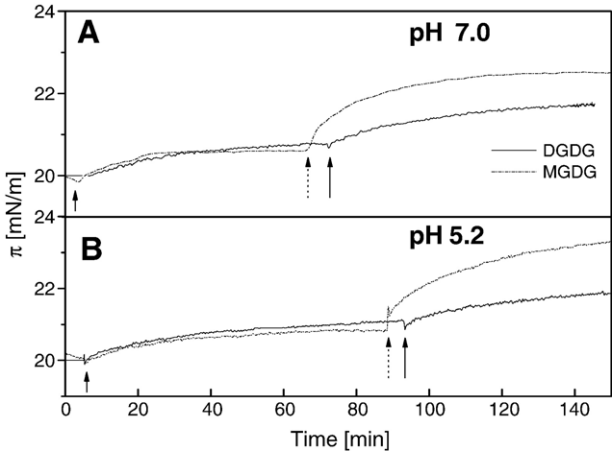

Fig. 2. Effect of pH on interaction between wheat FNR and MGDG or DGDG monolayer (air–water interphase), as monitored by changes in the surface pressure. A—pH 7.0, B—pH 5.2. Arrows indicate injection of the enzyme beneath monolayer (solid—DGDG monolayer, dotted—MGDG monolayer).

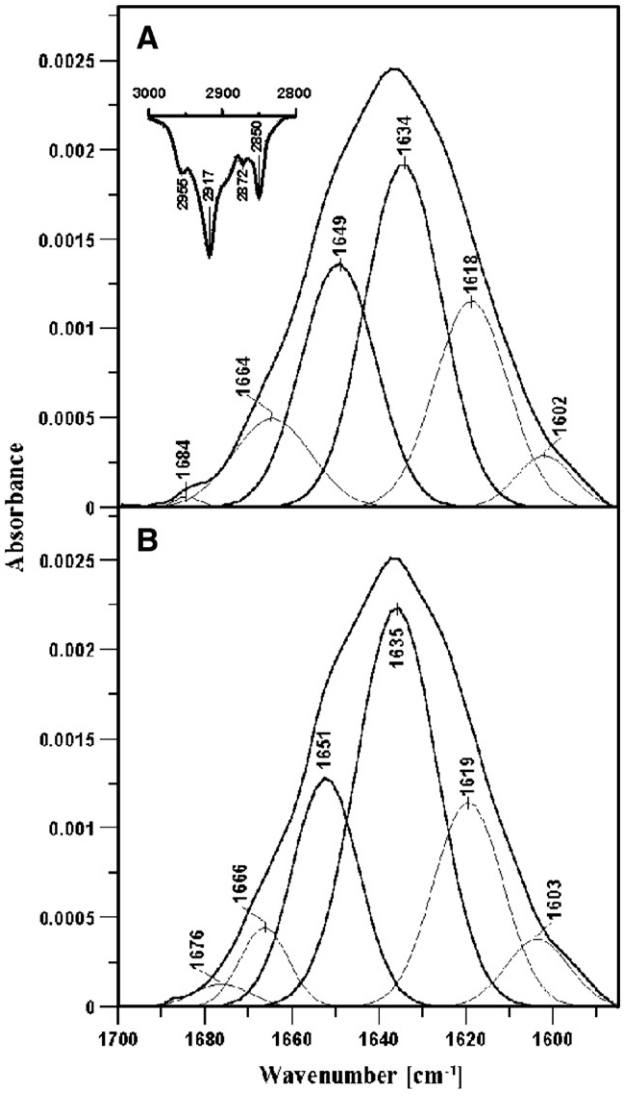

Fig. 3. FTIR spectra of the FNR incorporated to DGDG bilayer on water phase buffered with 25 mM HEPES/NaOH pH 7.0; A—spinach protein, B—wheat protein. Insert—the changes in the region 3000–2800 cm^{-1}.

2.6. Circular dichroism

CD spectra were measured with a Jasco 710 Spectropolarimeter (Jasco, Research Ltd.) in the range 180–260 nm, scan speed 10 nm/min, 5 scans accumulation. FNR stock solution was dialysed against a 25-mM HEPES buffer pH 7.0. 25 μl of dialysed stock solution was mixed with 275 μl of the respective buffer (25 mM HEPES/NaOH pH 7.0 or 8.2, or 25 mM Mess/NaOH pH 5.2). For the CD spectra in presence of liposomes, the SUV in respective buffer were added. Spectra were analyzed by JFit program with poly-L-lysine as reference [34].

2.7. FNR activity assays

The NADPH-dependent reduction of DBMIB (diaphorase reaction) was used in the study of FNR activity. The reaction assay consisted of 0.1 mM NADPH, 25 μM DBMIB and 0.02 μM FNR in 40 mM Tris/HCl buffer pH 8.7 in a total volume of 2 ml. The reaction was started by enzyme addition. The oxidation of NADPH was recorded spectrophotometrically using a DW2000 SLM Aminco® (USA), as decreasing at $\lambda = 340$ nm (absorption maximum of reduced form of NADP, $\varepsilon = 6.22\ mM^{-1}\ cm^{-1}$). To investigate the changes in FNR activity after the binding of lipids, the enzyme was preincubated for 30 min with SUV, and then the whole mixture was used to start the reaction.

2.8. Other procedures and chemical

A Laemmli SDS-PAGE [35], with 12% acrylamide was performed on 10×6 cm plates. Gels were stained with Coomassie Briliant Blue R-25 or by a silver staining procedure. Native electrophoresis with 12% acrylamide was performed on 10×6 cm or 22×18 cm plates. Staining for NADPH-dependent diaphorase activity was performed by the incubation of the gel for 1 h in darkness in 1 mM dichlorophenol indophenol, 0.01 mM 3-(4,5-dimethylthiazol-2-yl)-2,5-diphenyltetrazoliumbromide salt and 0.5 mM NADPH in 40 mM Tris/HCl buffer pH 8.7 (modified from [36]).

Protein concentration was determined with Bradford assay (Sigma Co), with a bovine serum albumin calibration curve. The water used for spectrophotometric and monolayer experiments was MiliQ quality. MGDG and DGDG came from Lipid Products, GB. NADPH, DBMIB and spectrophotometrically pure HEPES, were from Sigma, Co. Other chemicals came from Polskie Odczynniki Chemiczne, Poland, and were of analytical grade.

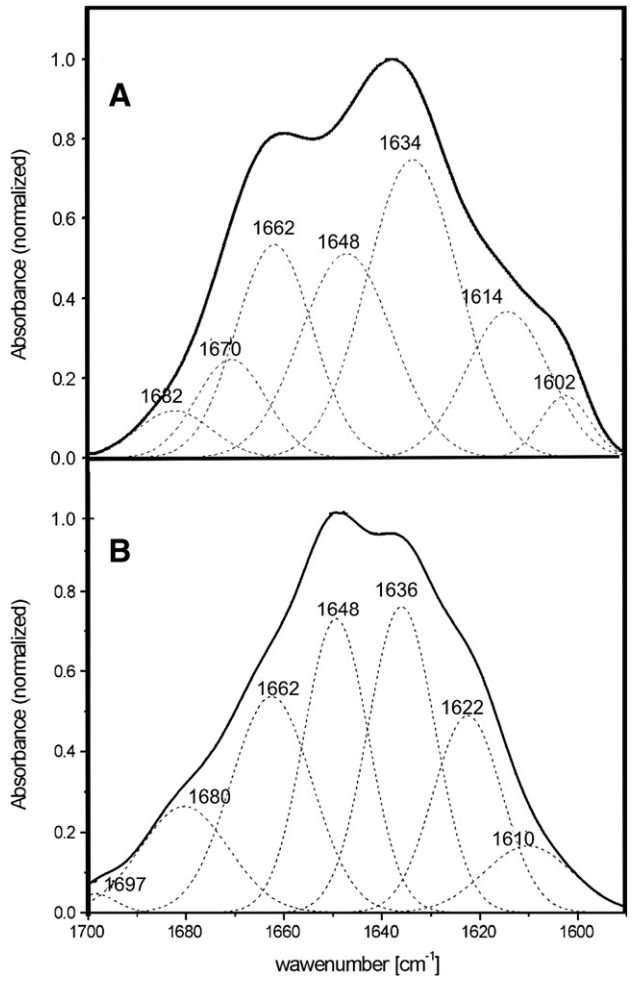

Fig. 4. FTIR spectra of FNR as partially hydrated film on ZnSe plate. A—spinach and B—wheat enzyme.

Table 2
The results of amide I band deconvolution for described variants of experiment (assignment due to [47,48])

Band position [cm^{-1}]	Area [%]	Band position [cm^{-1}]	Area [%]	Possible band assignment
Spinach FNR		Wheat FNR		
The enzyme deposited on ATR by means of evaporation				
1682	2,4	1698	0,88	β-sheet (second frequency)
1671	7,48	1680	10,88	Turn
1662	19,07	1662	20,23	Coil
1647	21,14	1649	21,76	α-helix
1634	30,11	1636	23,73	β-sheet (main frequency)
1614	15,73	1622	15,72	Aggregated protein
1602	3,8	1610	6,8	Side-chain
The enzyme incorporated into DGDG bilayer, pH 7.0				
1684	0,41	1676	1,84	Turn (second frequency)
1664	9,90	1666	5,43	Turn (main frequency)
1649	26,11	1651	21,89	α-helix
1634	37,82	1635	44,66	β-sheet (main frequency)
1618	21,61	1619	20,14	Aggregated protein
1602	4,14	1603	6,04	Side-chain

3. Results

3.1. Interaction of FNR with lipids — monolayer experiment

To investigate if an FNR molecule could directly bind to lipid molecules, a monolayer experiment was performed. DGDG and MGDG had been chosen as two main lipids of thylakoid membranes. The isotherms of compression showed that the area of the head group of both lipids was similar and did not depend on the pH of the water phase. For both lipids, an injection of spinach FNR (final concentration 67 nM) to a solution under the monolayer resulted in an increase in surface pressure. At pH 7, there was almost no difference in the rate and maximal level of the increase (Fig. 1A). At pH 5.2 the rate of FNR binding to the monolayer was higher for both tested lipids, and for MGDG the increase was significantly higher than for DGDG (Fig. 1B). For pH 8.2 the description of the process was comparable to pH 7.0 (not shown). In all conditions, a second injection of the enzyme resulted in a slower and less significant increase in surface pressure (not shown). After a period of about 1 h the surface pressure started to decrease and reached values lower than under starting conditions (not shown).

The rate of binding in dependence of lipid and pH could be ordered as follows: MGDG-5 > DGDG-5 > MGDG-7 = DGDG-7 = MGDG-8 = DGDG-8. It might be of interest to note that the rate and level of surface pressure changes depended on the starting pressure, and were higher for a lower starting point (not shown).

For wheat FNR the increase in surface pressure after injection under the DGDG or MGDG monolayer has been also shown. However, the first injection (to a final concentration 10 nM) resulted in a slow increase in π. The second injection (to a final concentration of 20 nM FNR), unlike the second injection of spinach FNR, gave an over additive increase in π. The rate of the increase in surface pressure after second injection could be ordered in a different manner than the same scheme as for spinach FNR — the fastest for MGDG, pH 5, slower for MGDG pH 7.0, and slowest for DGDG pH 5.2 or MGDG in pH 7 (Fig. 2).

3.2. FTIR spectra of FNR in bilayer

To check if FNR could incorporate into the lipid membrane the FTIR spectra were recorded. A bilayer formed of DGDG in buffer pH 7.0 or 8.2 was used. The quality of the bilayer was checked by a calculation of the dichroic ratio for C–H stretching vibrations in CH_2 and CH_3 groups (Table 1). DGDG was chosen due to its bilayer forming properties. Both for spinach FNR (Fig. 3A) and wheat FNR (Fig. 3B), after injection under the bilayer, amide I and amide II bands appeared. The intensity of these bands increased with time, indicating a time scale similar to experiments on the monolayer. Interestingly, in the region of 3000–2800 cm^{-1}, representing the C–H stretching vibrations in CH_2 and CH_3 groups, in the course of the experiment, the intensity decreased and minima were observed (Fig. 3, insert). The deconvolution of the amide I band showed the highest

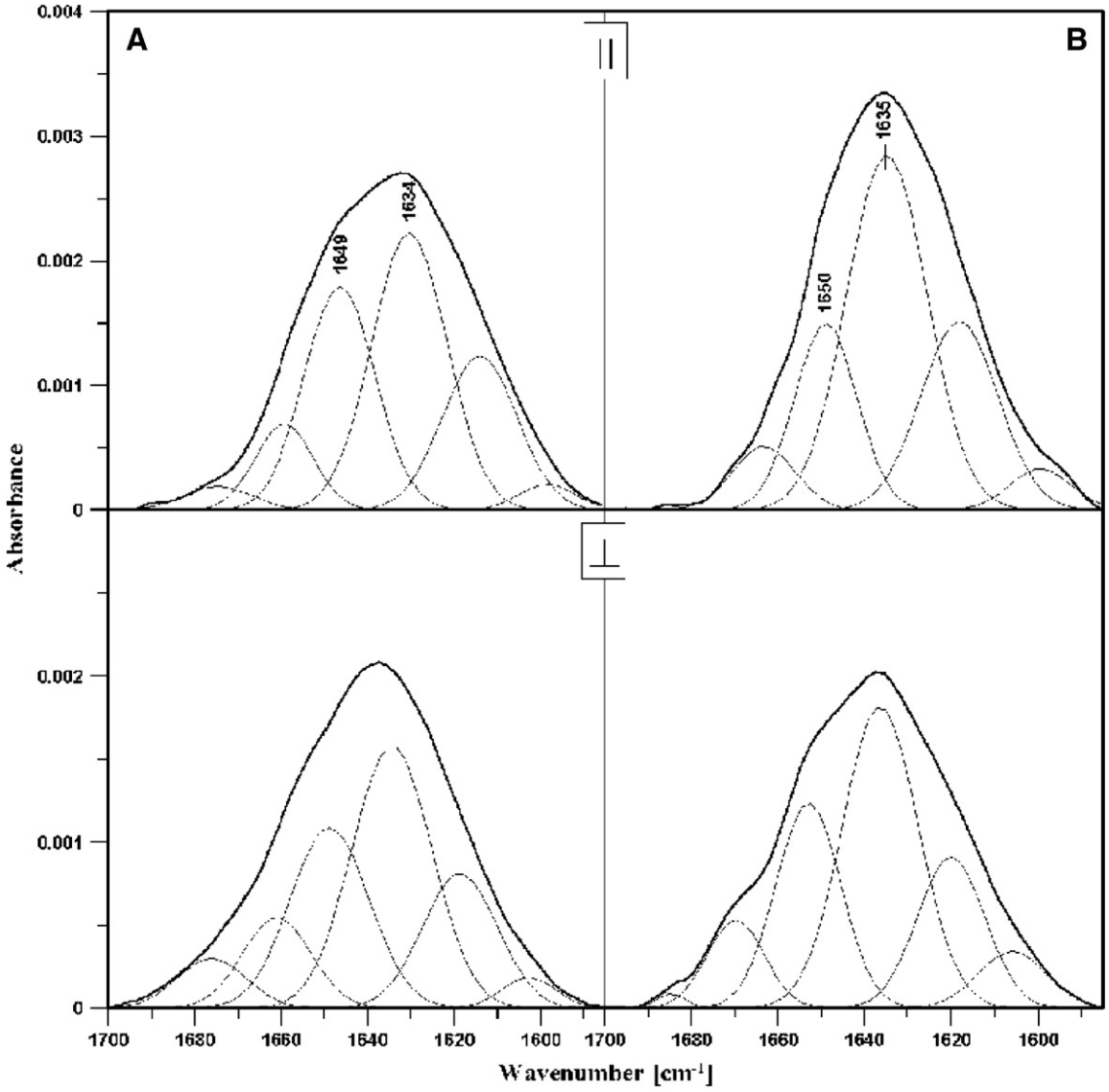

Fig. 5. Deconvolution of IR spectra recorded with polariser, for FNR in DGDG bilayer formed of water phase, buffered with 25 mM HEPES/NaOH pH 7.0. Orientation of electric vector indicated in the figure. A—spinach FNR, B—wheat FNR.

Table 3
Orientation of secondary structure elements of FNR molecule in DGDG bilayer

FNR in DGDG		Band position [cm^{-1}]	Dichroic ratio R	Order parameter S	α [deg]	θ [deg]
Spinach	β-sheet	1634	1.27	0.47	90	36
	α-helix	1649	1.41	−0.31	34	69
Wheat	β-sheet	1635	1.66	0.11	90	51
	α-helix	1650	1.22	−0.50	34	88

intensity for a band at 1635 cm^{-1}. As a control, the spectra of partially hydrated FNR (spinach or wheat), deposited to ZnSe crystal by means of evaporation (a hydrated film) were recorded (Figs. 4A and B). The main band for partially hydrated spinach FNR was at 1634 cm^{-1}. Table 2 presents the detailed results of amide I deconvolution for all described variants of the experiment.

For a determination of the arrangement of the FNR molecule in relation to the membrane, the IR absorption spectra were recorded with an electric vector of radiation parallel and perpendicular to the plane of incidence (Fig. 5). The calculated average angles, formed by the main elements of the secondary structure of the protein, are shown in Table 3.

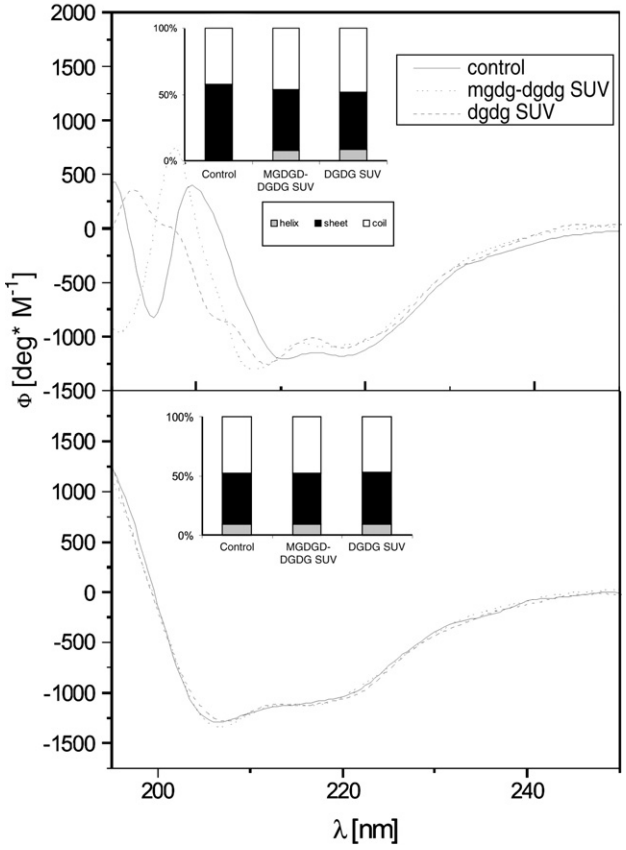

Fig. 6. Lipid induced changes in circular dichroism of spinach FNR in two different pH (A—7.0 and B—5.2). The concentration of FNR was 0.2 mg/ml, and FNR:lipid ratio was 1:15. Inserts—secondary structure composition, as calculated by JFit algorithm.

3.3. Secondary structure of spinach FNR in lipid environment as examined by circular dichroism

To determine the extent of the influence of the lipid environment on FNR secondary structure, the CD spectra of the enzyme were recorded in presence of small unilamellar liposomes, consisting of 100% DGDG or 30% MGDG and 70% DGDG. The spectra recorded for pH 7 are shown in Fig. 6A. Analysis with the JFit algorithm [34] showed a domination of β-sheet. Almost no α-helix structure was detected. The interaction with lipids (both MGDG and DGDG) caused a conversion from β-structure to α-helix of about 10% of protein (Fig. 6A, insert). In pH 5.2 the secondary structure of FNR was enriched in α-helix. Interaction with lipids did not cause an alteration in the spectra (Fig. 6B). The JFit error of fitness was in the range 11–15%.

3.4. The dimension of FNR molecule in dependence of pH

To compare the dimension of spinach FNR molecule in two different pH (7.0 and 5.2) a monolayer of protein was formed and compressed. The isotherms of compression are shown in Fig. 7. In both pH, a two phase increase in surface pressure was observed and two values of area might be distinguished. In pH 5.2 the calculated areas were almost two times higher than in pH 7.0.

3.5. The influence of lipids on FNR activity

To determine if interaction with lipids has any influence on the enzymatic properties of FNR, the NADPH-dependent reduction of DBMIB was tested. The FNR activity after control incubation was lower when compared to the situation without that treatment, what might be referred to an unknown mechanism related to lack of stabilizing properties of Tris (not shown, also mentioned in [37]), replaced by HEPES in this experiment, and in a less extent to the partial refolding of

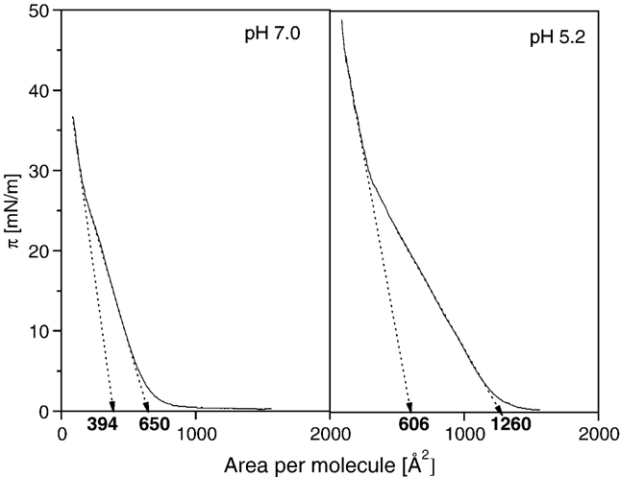

Fig. 7. Isotherms of compression of monomolecular layer of spinach FNR on air–water interphase, in pH 7.0 and pH 5.2. The calculated areas per molecule are indicated.

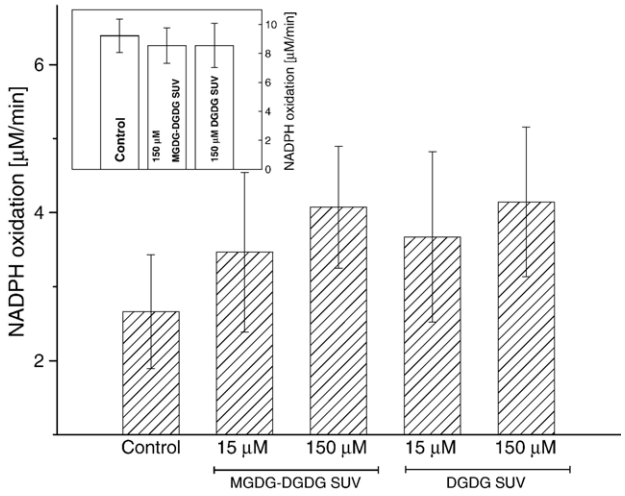

Fig. 8. Spinach FNR activity after 30 min incubation with 30% MGDG–70% DGDG liposomes or 100% DGDG liposomes. Insert—the activity of FNR without preincubation. Concentration of lipids indicated in the figure.

protein and destabilization of FAD binding. A 30-min preincubation (the time comparable to a maximal increase in surface pressure in monolayer experiments) with 100% DGDG SUV, or 30% MGDG–70% DGDG (mol%) SUV, caused an increase in activity, in comparison to the enzyme incubated without liposomes (Fig. 8). The activation was more significant for higher lipid concentrations and no difference between the two types of liposomes has been found. The presence of liposomes in the reaction medium, without previous incubation with the enzyme, caused the opposite effect. Activity decreased slightly, and as previously—no difference between effect of MGDG+DGDG containing liposomes, or pure DGDG vesicle has been recorded (Fig. 8, insert). Comparable behaviour was found for wheat FNR (not shown).

4. Discussion

In this work we have shown that FNR, both from spinach and from wheat, can interact with model membranes. The interaction influences the secondary structure of proteins, inducing conformational changes. As a consequence, enzymatic activity is also altered.

4.1. Binding to the membrane

Injection of FNR beneath the monomolecular layer of lipids resulted in an increase of surface pressure. The rise of π most probably came from the penetration of the enzyme molecule between lipid molecules. If so, part of a single FNR molecule had to interact with the head groups (sugar moieties) and perhaps additionally with the hydrophobic core of the membrane. It is hard to establish whether only first possibility occurs. Direct evidence coming from protein amide I band analysis in the FTIR spectra of the bilayer indicates that at least part of the protein molecule was incorporated into the membrane. The intensity of the amide I increased with time corresponding to the rise in surface pressure observed in the experiment with monolayers. There was no special difference in effects between monolayer and bilayer. Hence, the FNR molecule seems to interact with one layer only. Taking into consideration the dimension of FNR (for the crystal structure of spinach FNR, the longer axis is about 57 Å, shorter axis—37 Å, [5], and monolayer thickness (~20 Å), a great part of the enzyme might be still exposed to the water environment. If FNR could incorporate as integral protein, the NADPH-binding place would be hidden in lipids and inaccessible from hydrophilic environment, which would cause a decrease of activity and not the increase we reported. This assumption was confirmed by an observed difference in the amide I band of partially hydrated film of protein and the protein in bilayer, possibly resulting from less intensive absorption of the structure not incorporated into the bilayer. What is more, the observed decrease of surface pressure after longer times suggests that FNR might detach from the membrane, taking some lipid molecules away. A decline in the amount of lipid molecules was observed as a decrease of intensity in the FTIR spectrum region corresponding to the C–H stretching vibrational band in the CH_2 and CH_3 groups of lipid acyl chains. Comparable behaviour has been described for bovine serum albumin interacting with stearic acid monolayers [30]. The formation of specific BSA–lipid complexes resulted in the total removal of stearic acid from the air–water interphase.

The rate of FNR binding to the membrane was generally higher in pH 5.2 than in pH 7.0 or 8.2. In lower pH the interaction with the MGDG monolayer was higher than for DGDG. The dependence of FNR binding on proton concentration could not result from a change in lipid properties, because the isotherms of compression of MGDG and DGDG monolayers were comparable, also at various pH. The obtained areas per lipid molecule were almost the same, indicating that protein, when binding, recognizes the same galactosyl moiety in MGDG or DGDG. The easier connection to the MGDG monolayer might be the consequence of a tendency to form non-bilayer structure by this lipid, which facilitates protein incorporation [24], although lipid properties alone do not explain the observed variance in pH 5.2 and pH 7.0. A similar technique has been applied to describe the pH-dependent interaction of human annexins (the family of Ca^{2+} and lipid binding proteins) with phospholipids. The maximal increase of surface pressure was obtained for acidic pH. At neutral pH, the increase was ten times less. The pH-dependent changes resulted most probably from the protonation of several Asp and Glu residues and a slight increase of β-sheet and random coil [38].

In case of FNR, the difference in binding at various pH should also be the result of protein properties. The lowering of pH resulted in the exposition of the hydrophobic parts of the protein, suggesting that this is a factor determining the incorporation rate. Comparably, folding of apocytochrome c in lipid membranes was driven by a charge-dependent and hydrophobic lipid–protein interaction [39]. Leenhouts et al. [40] described the charge-dependent insertion of β-lactoglobulin into monoglyceride monolayers, facilitated after the addition of about 5–10%

of charged residues. However, both MGDG and DGDG are neutral lipids, and charge-dependent changes in the protein might be only a factor inducing direct hydrophobic contact between FNR and the membrane.

A higher rate of interaction with the membrane was observed in the case of wheat FNR as compared to spinach FNR, and this might have been a result of the different charges of these proteins. In the case of wheat FNR, in the investigated sample there was an isoform of theoretical pI 5.3, while the theoretical pI of spinach FNR is about 6.3. The pI on a native wheat enzyme is about 4.95 [17], and the pI of the spinach enzyme equals 5.3 [41]. Both spinach and wheat isoforms of FNR should be protonated in a comparable manner – with a net minus charge in pH 7.0 and a net zero charge in pH 5.2 – but there is a bigger number of charged residues within the wheat enzyme molecule. The over additive increase of π after a second injection, observed in the case of the wheat enzyme, possibly came from the wheat FNR is able to aggregate [17]. For the second portion of the injected protein molecules, establishing the connection was easier, because not only lipid–protein, but also protein–protein interactions were involved.

4.2. Secondary and tertiary structure of protein

In the crystal structure of spinach FNR, the secondary structure consists of 25% of α-helix, 27% of β-sheet and 48% of coil [5]. Yoshida et al. [41] applied FTIR spectroscopy to spinach FNR and for the protein in D_2O solution at neutral pH, they found the 20% of α-helix, 22% of β-sheet, 41% of coil and 18% of turns. The deconvolution presented in this work for spinach FNR in the form of "partially hydrated film" gives an amount of α-helix (22%), which fits well with above mentioned work, although the content of β-sheet was significantly higher (32%). The amount of turns was also the lower that obtained by [42]. Such a difference might be the result of lower stability of β-sheet in pH used for crystallisation (about 5 [5]). This assumption was proved by circular dichroism measurements at pH 7.0 and pH 5.2, and the observation that at lower pH less β-structure appeared. Moreover, the isotherms of compression of spinach FNR showed that the size of the protein molecule was significantly higher at pH 5.2 than at 7.0. The difference might come from the reorientation of two domains, resulting in a different angle and greater dimension. The shift in conformation might lead to the exposition of more hydrophobic amino acid residues. Such an answer to the higher concentration of protons is of great probability, because the FNR molecule is rich in lysine residues, located mainly at the outer surface of the protein, as deduced from crystal structure [5]. Poly-L-lysine, a synthetic peptide, has the tendency to adopt a different secondary structure in different pH conditions [43].

Conformational changes have been suggested for the light dependent regulation of FNR activity, in response to a decreasing proton concentration. Such a change resulted in changes of K_d for $NADP^+$ and K_m for NADPH and ferredoxin [44]. Conformational changes, induced by Fd or apoFd, facilitated binding of substrate, DBMIB [21]. Crystallographic studies of the FNR–Fd complex [3] have shown that structures of complex and free proteins differ in several ways, e.g. a new hydrogen bond is induced in the active center of FNR. Our results (both the circular dichroism spectra and the deconvolution of protein amide I band in the IR spectrum) showed that the secondary structure of FNR was changed also by lipids. A coil-assigned band in the IR spectra of membrane bound FNR was not detected. This might mean that lipids stabilized the more flexible parts of the protein. It is quite expected that lipids would so influence protein structure. Lad et al. [30] noted that during incorporation of lysozyme into the stearic acid monolayer the amide I peak increased, and was shifted to a slightly lower wavenumber, which corresponds to a reduction in α-helix structure and a small increase in random coil contents. But the absence of a coil band in the amide I region of FNR in the bilayer, also suggests that incorporation into the membrane occurs mainly via the β-structure regions of the protein. The obtained parameters, characterizing the orientation of β-structure and α-helix in the membrane are in agreement with this hypothesis. Both for spinach and wheat FNR, the average angle for helix suggests a near to perpendicular orientation to the normal of the membrane. A high content of β-structure might be found in the N-terminal domain of FNR (Fig. 9). A partial incorporation of this region into the membrane should not disturb catalytic activity, since most of its amino acid residues are not significant in the mechanism of catalysis. However, it might result in the immobilization of the protein and the facilitation of substrate

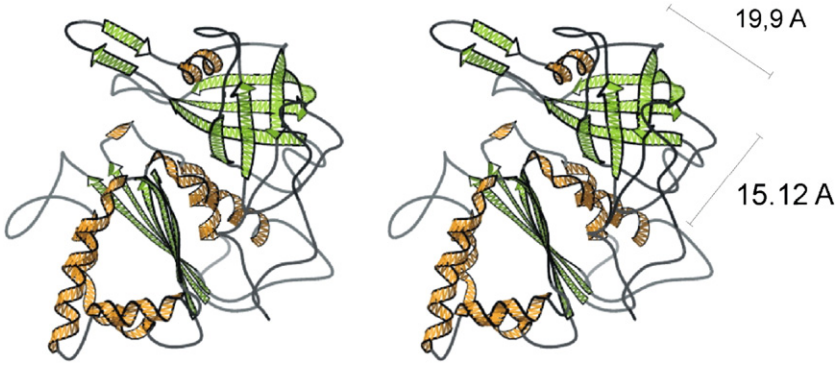

Fig. 9. Stereo view of spinach FNR (based on crystal structure 1FNB [5]).

binding, leading to an observed increase in FNR activity. The presence of liposomes in the reaction mixture without pre-incubation with enzyme slightly decreases the reaction rate. Most probably lipids act as scavengers for DBMIB radicals, formed during the reduction of this substrate [19]. The mechanism of lipid-induced DBMIB binding may be similar to that of the apoFd dependent increase in DBMIB reduction rate [19,20], involving the N-terminal, Fd-binding, flexible fragment of FNR [4].

In the CD spectra a decline in coil content was not detected. The CD results may differ from those obtained with FTIR, because in the first technique all FNR molecules are measured (both lipid bound and unbound), while in the second technique, only the membrane-bound FNR molecules are recorded. Interestingly, the lipids in pH 7.0 caused a change in the CD spectrum of FNR, making it similar to the FNR spectrum in pH 5.2 (both with or without lipids). This indicates that lipid–FNR interaction is related to proton concentration and its influence on the enzyme structure. Thus the first effect of lipid binding to FNR might be the charge-dependent change in the conformation of the protein.

4.3. Possible lipid binding sites on FNR molecule

The N-terminal domain of FNR forms a β-barrel motif with the hydrophobic niche [5], which should be big enough to bind a lipid molecule. A comparison of the lipid binding sites of β-lactoglobulin (22 Å × 20,7 Å, [45] with the dimension and shape of the respective sites on the FNR (Fig. 9) supports this assumption. However, this binding mode would be an explanation for interaction with a single lipid molecule, but it does not describe the incorporation of FNR into the membrane, especially as the first step in MGDG or DGDG binding should involve interaction with its hydrophilic sugar moiety. Although the full answer to this question demands more study, however the results presented in this paper permit a better understanding of the function of FNR *in vivo*. FNR is a water-soluble protein and up to now, its interaction with lipids has not been described. It is known that the enzyme could be incorporated into the micelles of sodium cholate and reduce plastoquinone [22], and it has been postulated that FNR might play a role in cyclic electron transfer in chloroplast [46]. Our work gives evidence that FNR incorporation into the thylakoid membrane *in vivo* should be possible. What is more, the wheat FNR isoform, which is probably mainly involved in cyclic electron transfer, was shown to connect the membrane more easily than spinach FNR. However, FNR isoforms participating in linear electron transport can also efficiently bind membrane. This suggests that the mechanism directing the enzyme to one of the two possible electron pathways involves pH-dependent protein conformational changes.

Acknowledgement

This work was financed from the Sources of Polish Minister of Science for the years 2004–2007 as the ordered research project No PBZ-KBN-110/PO4/19.

References

[1] A.K. Arakaki, E.A. Ceccarelli, N. Carrillo, Plant-type ferredoxin-NADP$^+$ reductase: a basal structural framework and a multipily of functions, FASEB J. 11 (1997) 133–140.
[2] N. Carrillo, F.A. Ceccarelli, Open questions in ferredoxin-NADP+ reductase catalytic mechanism, Eur. J. Biochem. 270 (2003) 1900–1915.
[3] G. Kurisu, M. Kusunoki, E. Katoh, T. Yamazaki, K. Teshima, Y. Onda, Y. Kimata-Ariga, T. Hase, Structure of the electron transfer complex between ferredoxin and ferredoxin-NADP$^+$ reductase, Nat. Struct. Biol. 8 (2001) 117–121.
[4] M. Maeda, Y.H. Lee, T. Ikegami, K. Tamura, M. Hoshino, T. Yamazaki, M. Nakayama, T. Hase, Y. Goto, Identification of the N- and C-terminal substrate binding segments of ferredoxin-NADP$^+$ reductase by NMR, Biochemistry 44 (2005) 10644–10653.
[5] C.M. Bruns, P.A. Karplus, Refined crystal structure of spinach ferredoxin reductase at 1.7 A resolution: oxidized, reduced and 2′-phospho-5′-AMP bound states, J. Mol. Biol. 247 (1995) 125–145.
[6] A. Aliverti, C.M. Bruns, V.E. Pandini, P.A. Karplus, MA. Vanoni, B. Curti, G. Zanetti, Involvement of serine 96 in the catalytic mechanism of ferredoxin-NADP$^+$ reductase: structure–function relationship as studied by site-directed mutagenesis and X-ray crystallography,, Biochemistry 34 (1995) 8371–8379.
[7] T. Jin, S. Morigasaki, K. Wada, Purification and characterisation of two ferredoxin-nadp$^+$ oxidoreductase isoforms from the first foliage leaves of mung bean (*Vigna radiata*) seedlings, Plant Physiol. 106 (1994) 697–702.
[8] S. Okutani, G.T. Hanke, Y. Satomi, G. Kurisu, A. Suzuki, T. Hase, Three maize leaf ferredoxin:NADP oxidoreductases vary in subchloroplast location, expression, and interaction with ferredoxin, Plant Physiol. 139 (2005) 1451–1459.
[9] G.T. Hanke, S. Okutani, Y. Satomi, T. Takao, A. Suzuki, T. Hase, Multiple iso-proteins of FNR in Arabidopsis: evidence for different contributions to chloroplast function and nitrogen assimilation, Plant Cell Environ. 28 (2005) 1146–1157.
[10] H.C. Matthijs, S.J. Coughlan, G. Hind, Removal of ferredoxin:NADP$^+$ oxidoreductase from thylakoid membranes, rebinding to depleted membranes, and identification of the binding site,, J. Biol. Chem. 261 (1986) 12154–12158.
[11] N. Weber, H. Strotmann, On the function of subunit PsaE in chloroplast Photosystem I, Biochim. Biophys. Acta 1143 (1993) 204–210.
[12] J.J. van Thor, T.H. Geerlings, H.C. Matthijs, K.J. Hellingwerf, Kinetic evidence for the PsaE dependent transient ternary complex photosystem I/Ferredoxin/Ferredoxin:NADP$^+$ reductase in a cyanobacterium, Biochemistry 38 (1999) 12735–12746.
[13] H. Zhang, J.P. Whitelegge, W.A. Cramer, Ferredoxin:NADP$^+$ oxidoreductase is a subunit of then chloroplast cytochrome b_6f complex, J. Biol. Chem. 276 (2001) 38159–38165.
[14] M.J. Quiles, J. Cuello, Association of ferredoxin-NADP oxidoreductase with the chloroplastic pyridine nucleotide dehydrogenase complex in barley leaves, Plant Physiol. 117 (1998) 235–244.
[15] M. Shin, H. Ishida, Y. Nozaki, A new protein factor, Connectein as a constituent of the large form of ferredoxin-NADP reductase, Plant Cell Physiol. 26 (1985) 559–563.
[16] M. Shin, How is ferredoxin-NADP reductase involved in the NADP photoreduction of chloroplast? Photosynth. Res. 80 (2004) 307–313.
[17] J. Grzyb, I. Rumak, P. Malec, M. Garstka, K. Strzałka, Two isoforms of ferredoxin:NADP+ oxidoreductase from wheat leaves—purification and initial biochemical characterisation. Submitted to Photosynth. Res.
[18] P. Joliot, A. Joliot, Cyclic electron transfer in plant leaf, Proc. Natl. Acad. Sci. U. S. A. 99 (2002) 10209–10214.
[19] M. Bojko, S. Więckowski, Diaphorase activity of ferredoxin:NADP$^+$ oxidoreductase in the presence of dibromothymoquinone, Phytochemistry 40 (1995) 661–665.
[20] M. Bojko, S. Więckowski, NADPH and ferredoxin:NADP$^+$ oxidoreductase- dependent reduction of quinones and their reoxidation, Phytochemistry 50 (1999) 203–208.
[21] M. Bojko, S. Więckowski, Three substrate binding site on spinach

ferredoxin:NADP$^+$ oxidoreductase. Studies with selectively acting inhibitors, Photosynthetica 39 (2001) 553–556.
[22] M. Bojko, J. Kruk, S. Więckowski, Plastoquinones are effectively reduced by ferredoxin:NADP$^+$ oxidoreductase in the presence of sodium cholate micelles. Significance for cyclic electron transport and chlororespiraion, Phytochemistry 64 (2003) 1055–1060.
[23] Y. Shahak, D. Crowther, G. Hind, The involvement of ferredoxin-NADP+ reductase in cyclic electron transport, Biochim. Biophys. Acta 636 (1981) 234–243.
[24] E. van den Brink-van der Laan, J.A. Killian, B. de Kruijff, Nonbilayer lipids affect peripheral and integral membrane proteins via changes in the lateral pressure profile, Biochim. Biophys. Acta 1666 (2004) 275–288.
[25] D. Latowski, H.E. Akerlund, K. Strzałka, Violaxanthin de-epoxidase, the xanthophyll cycle enzyme, requires lipid inverted hexagonal structures for its activity, Biochemistry 43 (2004) 4417–4420.
[26] R. Goss, M. Lohr, D. Latowski, J. Grzyb, A. Vieler, C. Wilhelm, K. Strzalka, The role of hexagonal structure forming lipids in diadinoxanthin and violaxanthin solubilization and de-epoxidation, Biochemistry 44 (2005) 4028–4036.
[27] R. Goss, D. Latowski, J. Grzyb, A. Vieler, M. Lohr, C. Wilhelm, K. Strzalka, Lipid dependence of diadinoxanthin solubilization and de-epoxidation in artificial membrane systems resembling the lipid composition of the natural thylakoid membrane, Biochim. Biophys. Acta 1768 (2007) 67–75.
[28] R.M. Epand, Lipid polymorphism and protein–lipid interactions, Biochim. Biophys. Acta 1376 (1998) 353–368.
[29] R.A. Demel, W. Jordi, H. Lembrechts, H. vam Damme, R. Hovious, B. de Kruijff, Differential interaction of apo- and holocytochrome c with acidic membrane lipids in model systems and the implications for their import into nitochondria, J. Biol. Chem. 7 (1989) 3988–3997.
[30] M.D. Lad, F. Birembaut, R.A. Frazier, R.J. Green, Protein–lipid interactions at the air/water interface, Phys. Chem. Chem. Phys. 7 (2005) 3478–3485.
[31] L. Silvestro, P.H. Axelsen, Infrared spectroscopy of supported lipid monolayer, bilayer and multibilayer membranes, Chem. Phys. Lipids 96 (1998) 69–80.
[32] L. Silvestro, P.H. Axelsen, Membrane-induced folding of cecropin A, Biophys. J. 79 (2000) 1465–1477.
[33] H. Hasumi, E. Nagata, S. Nakamura, Molecular heterogenity of ferredoxin: NADP$^+$ reductase from spinach leaves, Biochem. Biophys. Res. Commun. 110 (1983) 280–286.
[34] E.L. Altshuler, N.V. Hud, J.A. Mazrimas, B. Rup, Random coil conformation for extended polyglutamine stretches in aqueous soluble monomeric peptides, J. Pept. Res. 50 (1997) 73–75.
[35] U.K. Laemmli, Cleavage of structural proteins during the assembly of the head of bacteriophage T4, Nature 227 (1970) 680–685.
[36] S.D. Tanksley, T.J. Orton (Eds.), Isozymes in plant genetics and breeding, Part A, Elsevier, Amsterdam, 1986.
[37] G. Zanetti, G.G. Forti, On the reactivity of the sulphydryl groups of ferredoxin nicotinamide adenine dinucleotide phosphate reductase, J. Biol. Chem. 244 (1969) 4757–4780.
[38] M. Golczak, A. Kirilenko, J. Bandorowicz-Pikula, B. Desbat, S. Pikula, Structure of human annexin a6 at the air–water interface and in a membrane-bound state, Biophys. J. 87 (2004) 1215–1226.
[39] E.A. Bryson, S.E. Rankin, E. Goormaghtigh, J.M. Ruysschaert, A. Watts, T.J.T. Pinheiro, Structure and dynamics of lipid-associated states of apocytochrome c, Eur. J. Biochem. 267 (2000) 1390–1396.
[40] J.M. Leenhouts, R.A. Demel, B. de Kruijff, J.W.P. Boots, Charge-dependent insertion of b-lactoglobulin into monoglyceride monolayers, Biochim. Biophys. Acta 1330 (1997) 61–70.
[41] G. Zanetti, D. Cidaria, B. Curti, Preparation of apoprotein from spinach ferredoxin-NADP+ reductase. Studies on the resolution process and characterization of the FAD reconstituted holoenzyme, Eur. J. Biochem. 126 (1982) 453–458.
[42] S. Yoshida, Y. Toshitsugu, K. Shirabe, M. Takeshita, Analyses by Fourier transform infrared spectroscopies of protein structure of soluble NADH-cytochrome b5 reductase prepared by site-directed mutageneses: comparison with ferredoxin-NADP+ reductase, Biospectroscopy 3 (1996) 215–223.
[43] N. Greenfield, G.D. Fasman, Computed circular dichroism spectra for the evaluation of protein conformation, Biochemistry 8 (1969) 4108–4116.
[44] N. Carrillo, R.H. Valejos, Essential histidyl residues of ferredoxin-NADP+ oxidoreductase revealed by diethyl pyrocarbonate inactivation, Biochemistry 22 (1983) 5889–5897.
[45] L. Sawyer, G. Kontopidis, The core lipocalin, bovine beta-lactoglobulin, Biochim. Biophys. Acta. 1482 (2000) 136–148.
[46] M. Lintala, Y. Allahverdiyeva, H. Kidron, M. Piippo, N. Battchikova, M. Suorsa, E. Rintamaki, T.A. Salminen, E.M. Aro, P. Mulo, Structural and functional characterization of ferredoxin-NADP+-oxidoreductase using knock-out mutants of Arabidopsis, Plant J. 49 (2007) 1041–1052.
[47] E. Goormaghtigh, V. Cabiaux, J.M. Ruyssachaert, Secondary structure and dosage of soluble and membrane proteins by attenuated total reflection Fourier-transform infrared spectroscopy on hydrated films, Eur. J. Biochem. 193 (1990) 409–420.
[48] S. Wi, P. Pancoska, T.A. Keiderling, Prediction of protein secondary structure using factor analysis on Fourier transform infrared spectra: effect of Fourier self-deconvolution of the amid I and amid II bands, Biospectroscopy 4 (1998) 93–106.